

Structural models and core-level shifts of the oxidation of the Si(001) surface

J. T. Arantes, R. H. Miwa, and T. M. Schmidt

Faculdade de Física, Universidade Federal de Uberlândia, CP 593, CEP 38400-902, Uberlândia, MG, Brazil

(Received 10 February 2004; revised manuscript received 13 August 2004; published 17 December 2004)

A first-principles investigation of the oxygen adsorption processes on the Si(001) surface is presented. Our optimized full core potential calculations give nine energetically stable structural models for the suboxide Si¹⁺, Si²⁺, and Si³⁺ components. Our computed initial state Si 2*p* core-level shifts for the most stable configuration, of each Si^{*n*+} species, gives -0.96, -1.89, and -2.28 eV for *n*=1, 2, and 3, respectively. These results are in good agreement with high-resolution photoemission spectra, which allow us to determine the structural model of each Si^{*n*+} species. Also we verified a connection between the adsorption energies of the structural models and the measured intensity ratios of each suboxide component. The calculated adsorption energies of the most stable structural model for each species, in decreasing order, are Si²⁺, Si¹⁺, and Si³⁺, in agreement with experimental intensities for low O₂ dose results.

DOI: 10.1103/PhysRevB.70.235321

PACS number(s): 81.65.Mq, 79.60.Bm, 73.20.Hb

I. INTRODUCTION

The study of the oxidation on Si surfaces is important due to the vast technological applications of this material and the Si oxides.¹ An important issue in the oxidation process is the energetics and its connection with the stable adsorption sites of the oxygen adatom. For the oxygen chemisorption onto the top layer as well as on the first subsurface layer, scanning reflection electron microscopy measurements suggest a barrierless process at room temperature.² The oxidation of subsurface layers and the evolution of the innermost Si layers, which determine the oxide film growth, have been subject of important theoretical and experimental investigations.²⁻⁵ Concerning the initial process of Si(001) surface oxidation, recent Si 2*p* core-level investigations^{3,5} indicate the formation of multiply bonded Si surface nuclei, viz., Si¹⁺, Si²⁺, Si³⁺, and Si⁴⁺ species, even for low concentration of O adatoms. Such a result is in contrast with early experimental work,⁶ also based upon Si 2*p* core-level measurements, where the authors claimed that only the Si¹⁺ species is verified for low concentrations of O adatoms.

Many high-resolution Si 2*p* core-level shift data have defined the Si 2*p* binding energy shift for the Si¹⁺, Si²⁺, Si³⁺, and Si⁴⁺ species.^{3,7-10} However, the resolution of the core-level shift with respect to the local atomic configuration for each species is still not well understood. Different from the Si(001)/SiO₂ interface, where the calculated energetics, geometry, and the core-level shifts^{13,14} compare well with the experimental results,^{11,12} the oxidation on the Si(001) surface is not conclusive.

In this work, after a systematic analysis of the calculations obtained by different cluster and supercell methods and comparison with experimental data, we find a methodology based on the cluster approach that describes appropriately the Si(001) surface and the O₂ molecule. Then, in agreement with previous calculations,⁵ we verified that before the dissociation of the O₂ molecule, a triplet-to-singlet spin conversion occurs for an adiabatic oxidation. If the process is diabatic, the energy barrier can be reduced, depending on the O₂ incident energy, and the spin triplet is kept after the dis-

sociation of the molecule. In order to clarify the formation of oxygen nuclei on Si(001), we calculated the binding energy of the O adatom on the Si(001) surface, considering a number of different Si^{*n*+} geometries. We find four stable configurations for Si¹⁺, three configurations for Si²⁺, and two configurations for Si³⁺ species. The computed core-level shifts, for each (energetically most stable) configuration, are in good agreement compared with the experimental data.

II. METHOD OF CALCULATION

Our full core potential calculations are performed in the framework of the density functional theory (DFT),¹⁵ using a cluster method, where the potential energy hypersurface is obtained by a full geometry optimization (with no constrained degrees of freedom). The spin polarized DFT computations are carried out using the polarized split valence-type basis set 6-31G*. Tests of the convergence on the basis set and energy functionals have been done. The exchange-correlation energy is based on the Becke¹⁶ and Perdew-Wang formulation (PW),¹⁷ where a hybrid three-parameter exchange functional with a linear combination of Hartree-Fock, local, and gradient-corrected terms are combined with gradient-corrected correlation functional (B3PW91), as implemented in the GAUSSIAN94 computational code.¹⁸ This methodology has been shown to be very accurate to describe the O atom and the O₂ molecule parameters. The calculated O₂ binding energy is 5.44 eV, which is in good agreement with the experimental value 5.11 eV, and the optimized equilibrium bond length is 1.21 Å, which is exactly the experimental one. The electronic and structural properties of the clean Si(001) surface are also correctly described as will be discussed in the next section.

Since we have performed a full core calculation, the initial state contribution of the core-level shift has been calculated by comparing the single-particle energy eigenvalues of core states localized on different chemical environments. For instance, the surface (initial state) core-level shift is equal to the difference between the energy eigenvalues between a core state from a surface atom and the same core state from

a bulk atom. It is well known that the experimental core-level shifts are obtained by measuring the kinetic energy of photoexcited electrons; thus the core-hole relaxation is expected to occur: the final state contribution, which is not included in the single-particle energy difference. Pehlke and Scheffler¹⁹ proposed a correction to get the final state contribution by adding a total energy difference of a system with and without a core electron. Calculations of the core-level shifts, including the final state, have been performed for the Si(001) surface¹⁹ and Si(001)/SiO₂ interface.¹⁴ As the two calculations above are performed using the pseudopotential approach, where the core electrons are not explicitly considered, the initial states are calculated by different ways. The first one¹⁹ uses the average difference of the effective potential centered at different atoms, while the second one¹⁴ obtains the shift by first-order perturbation theory. The core-hole corrections in these two calculations, in general, have been shown to be overestimated, except for the Si up dimer of the Si(001) clean surface.¹⁹

For the Si(001) surface, the initial state contributions to the Si 2*p* core-level shifts were obtained by comparing the single-particle energy eigenvalues of a Si atom at the surface and a Si atom at the bulk position. For the reference bulk Si atom we choose the one at the most centering position of the cluster. As we have stated previously, we did not include any core-hole relaxation correction. For the Si up dimer atom of the clean Si(001) surface, the shift obtained using pseudopotential calculations is 0.25 eV and 0.48 eV for the initial and final states, respectively.¹⁹ Our results for the initial state is 0.56 eV, while the experimental one is 0.5 eV.^{3,20} The agreement between our initial state result with the measured one is also observed for the shifts of the different Siⁿ⁺ geometries, as will be shown in the next section.

III. RESULTS AND COMMENTS

A. The Si(001) clean surface

Although the Si(001) surface is, certainly, the most extensively studied surface,^{21,22} we will first carefully describe the clean Si(001) surface. By using first-principles calculations, especially in the DFT approach using supercell with slabs,^{23–25} the asymmetric dimerization of the Si surface atoms is shown to be an energetically favorable process. This buckling leads to the formation of lower symmetry patterns, the asymmetric (2 × 1), *p*(2 × 2), and *c*(4 × 2) systems, lowering the total energy in this order.^{23,26}

For cluster methods, some controversial remains. Clusters containing just one dimer, Si₉H₁₂, usually no Si-dimer buckling is observed using the local density approximation (LDA) or LDA with gradient corrections (PW91),²⁴ complete active space self-consistent-field (CASSCF),²⁷ and even including correlation with a multiconfiguration calculation (MCSCF).²⁸ Increasing to three the number of Si dimers on the surface, a buckling angle around 18° for the central dimer is observed using the LDA and PW91,²⁴ and no buckling is obtained using the MCSCF method. Using a three-parameter exchange energy functional (B3LYP),^{29,30} a different picture is observed. By using a 6-31G basis set with polarized functions a small buckling has been obtained, even for the cluster

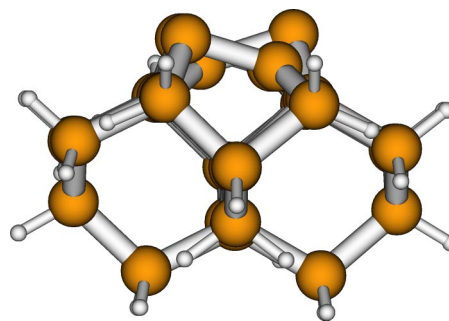


FIG. 1. (Color online) The Si₂₉H₂₈ cluster used in the calculation.

containing just one dimer on the surface,³¹ and increasing the cluster size the buckling also increases reaching 15°.

The experimental results also present some controversy. Different techniques^{32–36} find that alternating buckled dimers *p*(2 × 2) or *c*(4 × 2) reconstructions are formed. However, recent scanning tunneling microscopy experiments at low temperature observed that symmetric dimers dominate the surface.^{37,38} This apparently symmetric configuration can be explained by an anomalous flipping motion of the buckled dimers, as proposed by the authors.

So, based on the theoretical and experimental results some preliminary conclusions can be taken into account to describe the Si(001) surface by a first-principles calculation: (i) a basis set that permits a charge transfer between the two atoms in each dimer; (ii) the interaction between the dimers changes the structure, so clusters with more than one dimer are essential; (iii) the exchange and correlation energies have to be well described; and (iv) the relaxations have to be included at least until the third layer³⁹ (preferentially full optimization). Based on these findings we try to use a method that can match all items above.

We use the Si₂₉H₂₈ cluster with three dimers on the top surface as illustrated in Fig. 1. This three-dimer cluster has a symmetry where the second and third layers contain tetrahedral Si bonds. All calculations have been done including all electrons with no constraints in the optimization process. Basis sets have been tested to reproduce the charge transfers, and the best one found is the polarized split valence-type basis set 6-31G*. Our analysis shows that the hybrid three-parameter exchange-correlation functional, B3PW91, is the most appropriate one giving a Si-dimer buckling of 20.5° and 17.0° for the central and lateral dimers, respectively. The energy gain due to the buckling process is 0.15 eV/dimer, and the buckled dimer bond lengths are 2.31 and 2.27 Å for the central and lateral dimers, respectively. These results are in quite good agreement with the previous theoretical results, within the supercell (DFT) approach.^{23,25,26,40} In Table I we summarize our results for the Si(001) clean surface, where we also included the results for spin triplet for the dimers, which only occur without the Si-dimer buckling, being less favorable than the spin singlet. However, it is interesting to note that there is a spin contamination for the nonbuckling system. The difference between the singlet and the triplet is favorable for the triplet by 0.06 eV when the three dimers are symmetric, and with just the central dimer symmetric, the

TABLE I. Results for Si(001) clean surface. The energy ΔE is the energy difference with respect to the symmetric (nonbuckled) relaxed structure. M denotes the multiplicity, d is the dimer bond length, and α is the buckling angle.

	d (Å)	α (deg)
$\Delta E=0.00$ eV $M=1$		
central	2.20	0.0
lateral	2.12	0.0
lateral	2.12	0.0
$\Delta E=-0.44$ eV $M=1$		
central	2.31	20.5
lateral	2.27	17.0
lateral	2.27	17.0
$\Delta E=-0.06$ eV $M=3$		
central	2.39	0.0
lateral	2.22	0.0
lateral	2.22	0.0
$\Delta E=-0.12$ eV $M=3$		
central	2.38	0.0
lateral	2.25	14.3
lateral	2.25	14.3
$\Delta E=0.43$ eV $M=7$		
central	2.39	0.0
lateral	2.40	0.0
lateral	2.40	0.0

triplet is more stable by 0.12 eV, showing that the multiplicity is not an integer. This antiferromagnetic behavior has been suggested before, using tight-binding⁴¹ and recently in a DFT within the generalized gradient approximation.²³

For a symmetric dimer configuration, the dangling bonds on the surface form π and π^* combinations that come from the highest occupied molecular orbital (HOMO) and lowest unoccupied molecular orbital (LUMO), respectively. The buckling of the surface dimers leads to a mixing of the π and π^* orbitals and, consequently, increasing the HOMO-LUMO splitting, which in our calculation is 0.64 eV. This asymmetry of the dimers also provoke a rehybridization of the surface orbitals with a charge transfer from the lower to the upper Si atom, which is observed in our calculation. This electronic charge distribution leaves the lower atom with an sp^2 -like character, while the upper forms three tetrahedral bonds and a fully occupied dangling bond. This configuration opens up the electronic band gap, lowering the total energy of the system.

B. The energetics and the core-level shifts of the oxidation

Having a good description of the Si(001) clean surface and the O_2 molecule, we now turn to the oxidation processes. When the O_2 molecule approaches the surface, during an oxidation process, a dissociation of the O_2 molecule is expected before its adsorption on the Si surface. We search for stable (or metastable) adsorption sites for the O adatom onto

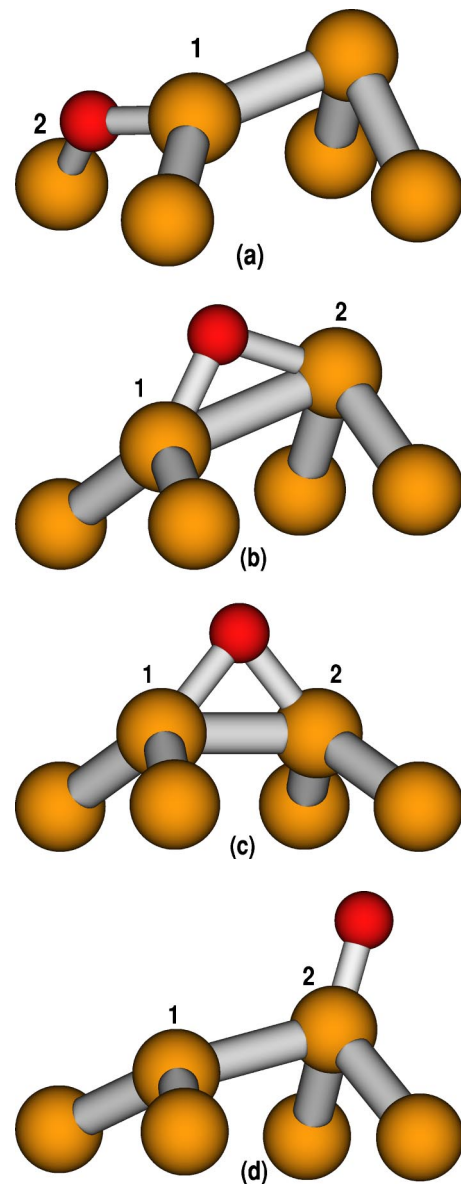


FIG. 2. (Color online) Stable sites for one O atom: (a) at the B site, (b) at the asymmetric Br site (Br1), (c) at the symmetric Br site (Br2), and (d) at the T site. The dark smaller ball represents the O atom.

the Si(001) surface. For each optimized structure containing n O atoms, we compute the adsorption energy (ΔE_i) with respect to free oxygen molecules as

$$\Delta E_i = E_i - \left[E_{\text{Si}(001)} + \frac{n}{2} E_{O_2} \right],$$

where E_i is the total energy of the configuration i , $E_{\text{Si}(001)}$ is the total energy of the Si(001) clean surface, and E_{O_2} is the energy of an isolated spin triplet O_2 molecule. All calculations, including the Si(001) clean surface and the O_2 molecule, have been performed using the same procedure: the same basis set, exchange-correlation, and convergence criterion. This ensures a direct comparison among the different configurations. We have considered a number of different

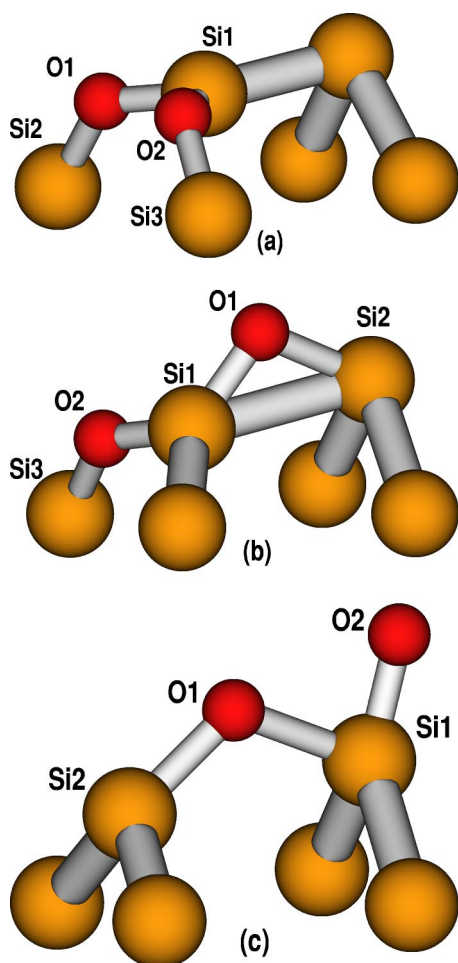


FIG. 3. (Color online) Stable configurations for two O atoms. (a) BB, both at B site, (b) BBr, one at the B site and the other at the Br site, (c) DT, one at the D site and the other at the T site. The dark smaller balls represent the O atoms.

atomic arrangements for the oxygen adsorption on the Si(001) surface.

Initially we considered the formation of the Si^{1+} suboxide structures. Our calculated adsorption energies indicate that the backbond site (*B*) of the Si down dimer atom is the energetically most favorable adsorption site for an O adatom, [Fig. 2(a)]. We find an adsorption energy of -6.90 eV per O_2 molecule. In this case, an O_2 molecule is dissociatively adsorbed on the Si(001) surface, giving rise to two Si^{1+} suboxides with the O adatom at the *B* site. The O adatom at the Si up dimer atom is unstable: a flipping of the buckled dimer occurs, becoming always a backbond down dimer configuration, which is in agreement with the theoretical investigation performed by Kato and Uda.⁵ The other atomic arrangements, buckled (Br1) and symmetric bridge bonds (Br2), shown in Figs. 2(b) and 2(c), respectively, are also energetically favorable structures. We find adsorption energies of -5.89 and -5.78 eV, respectively. The latter value of ΔE_i ($i=\text{Br2}$) is also in agreement with Kato *et al.*,⁴ who find 5.99 eV for an O_2 molecule dissociatively adsorbed at the bridge site. On the other hand, the dimer-bond (D) configuration, where the O atom stays between the two Si atoms of

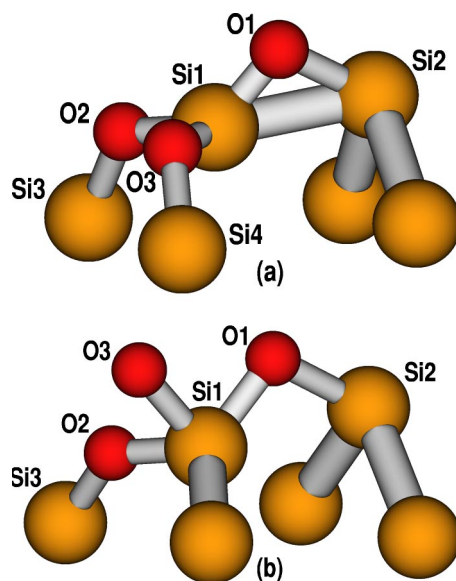


FIG. 4. (Color online) Stable configurations for three O atoms. (a) BBBr, two at the B site and one at the Br site, (b) BDT, one at the B site, another at D site, and the third one at the T site. The dark smaller balls represent the O atoms.

the top dimer making a bridge, differently from previous calculations,^{42,43} is unstable, and it drops in the Br2 configuration. Finally, the dangling-bond (T) configuration [shown in Fig. 2(d)] presents an adsorption energy of -3.91 eV. From our calculated values of ΔE_i for $i=\text{B}$, Br1, Br2, D, and T, we can infer the adsorption energies for mixed Si^{1+} complexes. For instance, an O_2 molecule adsorbed on Si(001) can give rise to two Si^{1+} suboxides with one O adatom at the *B* site and the other at the Br2 site. By computing the average value of ΔE_i for $i=\text{B}$ and Br2, we find an adsorption energy of -6.34 eV/ O_2 molecule. This result is in quite good agreement with the total energy investigation performed by Kato *et al.*,⁴ who obtained an adsorption energy of 6.16 eV/ O_2 molecule for the same Si^{1+} atomic configuration.

We next have considered the formation of Si^{2+} complexes on the Si(001) surface. For the adsorption of an O_2 molecule, the backbond of the same Si atom at the down position of the dimer (BB sites), Fig. 3(a), represents the energetically most stable configuration. In this case we have an adsorption energy of -7.02 eV/ O_2 molecule. We have also obtained two other stable configurations: (i) one O at the B site and another at the Br site (BBr), shown in Fig. 3(b), and (ii) one O at the D site and another at the T site (DT), shown in Fig. 3(c). The adsorption energies (per adsorbed O_2 molecule) are -6.53 (BBr) and -5.88 eV (DT). These results support the experimentally proposed BB1 and DT atomic configurations for Si^{2+} , proposed by Yeom *et al.*³ and Oh *et al.*¹⁰ In contrast, we find that the atomic arrangements with (i) one O at the B site and another at the D site (BD), and (ii) one O at the B site and another at T site (BT), both suggested before,^{3,10} are energetically unstable.

For three O atoms adsorbed in the Si(001) surface, forming Si^{3+} structures (shown in Fig. 4), we obtained two energetically stable configurations, viz., (i) two O at the B site, and the third one at the Br site [BBBr, Fig. 4(a)] and (ii) one

TABLE II. Adsorption energies (in eV) per adsorbed O₂ molecule (ΔE_i) and geometrical parameters for all stable configurations. $d_{\text{Si-Si}}$ is the top layer Si—Si distance; $d_{\text{Si-O}}$ is the Si—O bond length. Also given are the top layer Si—Si buckling angle (α) and the Si—O—Si angle ($\Theta_{\text{Si-O-Si}}$). The distances are in Å and the angles in degrees.

1 O	B	Br1	Br2	T
ΔE_i	-6.90	-5.89	-5.78	-3.91
$d_{\text{Si-Si}}$	2.29	2.65	2.25	2.42
$d_{\text{Si1-O}}$	1.64	1.78	1.74	-
$d_{\text{Si2-O}}$	1.72	1.65	1.74	1.55
α	19.4	16.0	0.0	15.9
$\Theta_{\text{Si-O-Si}}$	132.7	101.0	80.8	-
2 O	BB	BBr	DT	
ΔE_i	-7.02	-6.53	-5.88	
$d_{\text{Si-Si}}$	2.27	2.67	3.09	
$d_{\text{Si1-O1}}$	1.62	1.72	1.54	
$d_{\text{Si1-O2}}$	1.62	1.80	1.74	
$d_{\text{Si2-O1}}$	1.72	1.62	1.62	
$d_{\text{Si3-O2}}$	1.72	1.62	-	
α	15.1	15.9	12.3	
$\Theta_{\text{Si1-O1-Si2}}$	132.0	137.7	133.7	
$\Theta_{\text{Si1-O2-Si3}}$	132.1	102.5	-	
3 O	BBBr	BDT		
ΔE_i	-6.56	-6.24		
$d_{\text{Si-Si}}$	2.27	3.14		
$d_{\text{Si1-O1}}$	1.62	1.74		
$d_{\text{Si1-O2}}$	1.61	1.68		
$d_{\text{Si1-O3}}$	1.62	1.54		
$d_{\text{Si2-O1}}$	1.77	1.60		
$d_{\text{Si3-O2}}$	1.70	1.74		
$d_{\text{Si4-O3}}$	1.72	-		
α	15.1	16.8		
$\Theta_{\text{Si1-O1-Si2}}$	96.4	140.1		
$\Theta_{\text{Si1-O2-Si3}}$	122.5	149.1		
$\Theta_{\text{Si1-O3-Si4}}$	151.6	-		

O at the B site, another at the D site, and the third at the T site [BDT, Fig. 4(b)]. We obtained adsorption energies per O₂ molecule of -6.56 eV (BBBr) and -6.24 eV (BDT). The experimentally suggested^{3,10} BBD arrangement, two O atoms at B site and one at D site is energetically unstable. The structural parameters and the adsorption energies for all (energetically) stable configurations are summarized in Table II.

Our results indicate that the formation energies of the Si¹⁺, Si²⁺, and Si³⁺ structures are very close to each other, as shown in Table II. Thus, we can expect the coexistence of Si¹⁺, Si²⁺, and Si³⁺ structures (even for low coverage of oxygen) during the initial stage of the surface oxidation, in accordance with Yeom *et al.*³ and Oh *et al.*¹⁰ Furthermore, based upon our calculated adsorption energies, we verify a (slight) energetic preference for the formation of the Si²⁺

TABLE III. Calculated Si 2*p* core-level shifts (in eV) for Si¹⁺, Si²⁺, and Si³⁺ stable configurations, and the corresponding minimum and maximum values obtained from different experiments (Refs. 3 and 7–10).

Si ¹⁺	B	Br1	Br2	T	Expt.
	-0.96	-0.76	-0.22	0.28	-0.9 to -1.0
Si ²⁺	BB	BBr	DT		
	-1.89	-1.96	-0.06		-1.7 to -1.9
Si ³⁺	BBBr	BDT			
	-2.28	-0.13			-2.4 to -2.6

structure followed by the Si¹⁺ and the Si³⁺ structures (Table II), thus confirming the recent experimental findings by Oh and co-workers. Their measured Si 2*p* photoemission spectra, during the initial stage of Si(001) oxidation process, exhibit the highest intensity for Si²⁺ species.¹⁰ We can also infer that the B configuration (Si¹⁺) is a good candidate as a precursor configuration to the formation of BB structure for Si²⁺, since the B→BB structural transition is energetically favorable by 0.12 eV per O₂ molecule. On the other hand, these two configurations (B and BB) cannot be considered as precursors to the formation of the BBBr (Si³⁺) structure. The B→BBBr (BB→BBBr) structural transition is energetically unfavorable by 0.34 eV (0.46 eV). However, the BBr arrangement can be a good candidate as a precursor structure to the formation of the triple-bonded BBBr arrangement. In this case, the BBr→BBBr transition is energetically favorable by 0.03 eV, and the BBBr arrangement can be obtained throughout an oxygen adsorption to the (second) backbond of the Si down dimer atom.

In order to complement our total energy findings, we have calculated the initial state contributions for the Si 2*p* core-level shift for the Si¹⁺, Si²⁺, and Si³⁺ structures. The core-level shifts are computed by the difference of the single-particle energy eigenvalue of an atom at the bulk position and an atom at the surface bonded to oxygen atom. We did not include any correction related to the response of the valence electrons to the creation of the core hole. In particular, for the Si(001)/SiO₂ interface, such a correction, by using a pseudopotential calculation, overestimates the core-level shift for the Si—O bonds.¹⁴ For each configuration, we choose only one Si atom from the top surface (that of the Si dimer) to compute the 2*p* level. Among the two Si top atoms we always choose the Si atoms labeled as 1 in Fig. 2 to compute the 2*p* level, except for the T configuration [Fig. 2(d)], where we choose the Si atom 2, since it is the only one bonded to an oxygen atom. When there are equivalent atoms, we choose the one that has the greatest shift. We do not perform average shifts. For the Br2 configuration the shifts of the Si1 and the Si2 are very similar to each other. For Si atoms not bonded to O atoms, the shifts are always smaller than those bonded to O atoms.

In Table III we present the Si 2*p* core-level shift for each Si^{*n+*} species for the energetically stable structures obtained in our calculation. The last column of this table shows the energy interval for the measured high-resolution Si 2*p* core-level spectra.^{3,7–10} It is worth pointing out that the best agree-

ment between our results and the experimental measurements are obtained for the energetically most stable configuration for each Si^{n+} species, which is B, BB, and BBBr for the Si^{1+} , Si^{2+} , and Si^{3+} , respectively (see adsorption energies in Table II). Particularly for the B and BB structures, the agreement is exactly inside the experimental range. These results suggest a reduced energy correction, due to the core-hole screening during the photoemission process for the Si^{1+} and Si^{2+} structures. For BBBr our calculated shift is lower than the experimental one, which can be explained by the fact that we compute each configuration isolated from each other. As has been verified, with the evolution of the oxidation, the Si^{3+} and Si^{4+} species form two-dimensional islands,¹⁰ which is not taken into account in our calculation.

IV. CONCLUSIONS

We use a cluster full core potential calculation method within the density functional approach to investigate oxidation on the Si(001) surface. We find four energetically stable configurations for the Si^{1+} species, three for the Si^{2+} species,

and two for the Si^{3+} species. Our calculated adsorption energies indicate an energetic preference to the formation of the Si^{2+} structure followed by the Si^{1+} and the Si^{3+} structures, within an energy range up to 0.46 eV per O_2 molecule. These results clearly support the formation of two-dimensional oxygen clusters, or multiply bonded surface Si atoms in the initial stage of the Si(001) oxidation process. Some possible precursor configurations to the formation of the Si^{2+} and Si^{3+} species have been inferred, based upon our total energy results. Finally, the computed Si $2p$ initial state core-level shifts for the energetically most stable structure of each Si^{n+} species are in good agreement with high-resolution photoemission spectra for the corresponding species. Thus, we can infer a reduced energy correction, due to the core-hole screening during the photoemission process of Si^{n+} species on the Si(001) surface.

ACKNOWLEDGMENTS

This work was supported by the Brazilian agencies FAPEMIG and CNPq. We also would like to thank the CENAPAD-MG/CO for computer time.

-
- ¹As a review see T. Engel, Surf. Sci. Rep. **18**, 91 (1993).
²Heiji Watanabe, Koichi Kato, Tsuyoshi Uda, Ken Fujita, Masakazu Ichikawa, Takaaki Kawamura, and Kiyoyuki Terakura, Phys. Rev. Lett. **80**, 345 (1998).
³H. W. Yeom, H. Hamamatsu, T. Ohta, and R. I. G. Uhrberg, Phys. Rev. B **59**, R10 413 (1999).
⁴Koichi Kato, Tsuyoshi Uda, and Kiyoyuki Terakura, Phys. Rev. Lett. **80**, 2000 (1998).
⁵Koichi Kato and Tsuyoshi Uda, Phys. Rev. B **62**, 15&3x2009;978 (2000).
⁶P. Morgen, U. Höfer, W. Wurth, and E. Umbach, Phys. Rev. B **39**, 3720 (1989).
⁷G. Hollinger and F. J. Himpsel, Phys. Rev. B **28**, 3651 (1983).
⁸A. Mascaraque, C. Ottaviani, M. Capozzi, M. Pedio, and E. G. Michel, Surf. Sci. **377–379**, 650 (1997).
⁹Y. Enta, Y. Miyanishi, H. Irimachi, M. Niwano, M. Suemitsu, N. Miyamoto, E. Shigemasa, and H. Kato, Phys. Rev. B **57**, 6294 (1998).
¹⁰J. H. Oh, K. Nakamura, K. Ono, M. Oshima, N. Hrashita, M. Niwa, A. Toriumi, and A. Kakizaki, J. Electron Spectrosc. Relat. Phenom. **114–116**, 395 (2001).
¹¹F. J. Himpsel, F. R. McFeely, A. Taleb-Ibrahimi, J. A. Yarmoff, and G. Hollinger, Phys. Rev. B **38**, 6084 (1988).
¹²M. T. Sieger, D. A. Luh, T. Miller, and T.-C. Chiang, Phys. Rev. Lett. **77**, 2758 (1996).
¹³W. Orellana, Antônio J. R. da Silva, and A. Fazzio, Phys. Rev. Lett. **90**, 016103 (2003).
¹⁴Alfredo Pasquarello, Mark S. Hybertsen, and Roberto Car, Phys. Rev. B **53**, 10 942 (1996).
¹⁵P. Hohenberg and W. Kohn, Phys. Rev. **136**, B864 (1964); W. Kohn and L. J. Sham, *ibid.* **140**, A1133 (1965).
¹⁶A. D. Becke, Phys. Rev. A **38**, 3098 (1988).
¹⁷J. P. Perdew, J. A. Chevary, S. H. Vosko, K. A. Jackson, M. R. Pederson, D. J. Singh, and C. Fiolhais, Phys. Rev. B **46**, 6671 (1991).
¹⁸M. J. Frisch *et al.*, Gaussian Inc., Pittsburgh, PA (1995).
¹⁹E. Pehlke and M. Scheffler, Phys. Rev. Lett. **71**, 2338 (1993).
²⁰E. Landemark, C. J. Karlsson, Y.-C. Chao, and R. I. G. Uhrberg, Phys. Rev. Lett. **69**, 1588 (1992).
²¹H. J. W. Zandvliet, Rev. Mod. Phys. **72**, 593 (2000).
²²J. A. Kubby and J. J. Boland, Surf. Sci. Rep. **26**, 61 (1996).
²³Óscar Paz, Antônio J. R. da Silva, Juan José Sáenz, and Emilio Artacho, Surf. Sci. **482–485**, 458 (2001).
²⁴E. Penev, P. Kratzer, and M. Scheffler, J. Chem. Phys. **110**, 3986 (1999).
²⁵A. Ramstad, G. Brocks, and P. J. Kelly, Phys. Rev. B **51**, 14 504 (1995).
²⁶J. Fritsch and P. Pavone, Surf. Sci. **344**, 159 (1995).
²⁷M. R. Radeke and E. A. Carter, Phys. Rev. B **54**, 11 803 (1996).
²⁸Beate Paulus, Surf. Sci. **408**, 195 (1998).
²⁹A. D. Becke, J. Chem. Phys. **98**, 5648 (1993).
³⁰C. Lee, W. Yang, and R. G. Parr, Phys. Rev. B **37**, 785 (1988).
³¹R. Konečný and D. J. Doren, J. Phys. Chem. **106**, 2426 (1997).
³²Cheng Yang, S. Y. Lee, and H. Chuan Kang, J. Phys. Chem. **107**, 3295 (1997).
³³W. S. Yang, F. Jona, and P. M. Marcus, Phys. Rev. B **28**, 2049 (1983).
³⁴B. W. Holland, C. B. Duke, and A. Paton, Surf. Sci. **140**, L267 (1984).
³⁵D. Badt, H. Wengelnik, and H. Neddermeyer, J. Vac. Sci. Technol. B **12**, 2015 (1994).
³⁶E. L. Bullock, R. Gunnella, L. Patthey, T. Abukawa, S. Kono, C. R. Natoli, and L. S. O. Johansson, Phys. Rev. Lett. **74**, 2756 (1995).
³⁷R. Felici, I. K. Robinson, C. Ottaviani, P. Imperatori, P. Eng, and P. Perfetti, Surf. Sci. **375**, 55 (1997).

- ³⁷Y. Kondo, T. Amakusa, M. Iwatsuki, H. Tokumoto, Surf. Sci. **453**, L318 (2000).
- ³⁸T. Yokoyama and K. Takayanagi, Phys. Rev. B **61**, R5078 (2000).
- ⁴⁰R. H. Miwa, Surf. Sci. **418**, 55 (1998).
- ⁴¹E. Artacho and Félix Ynduráin, Phys. Rev. Lett. **62**, 2491 (1989).

- ⁴²Yoshiyuki Miyamoto and Atsushi Oshiyama, Phys. Rev. B **41**, 12 680 (1990).
- ⁴³Toshihiro Uchiyama and Masaru Tsukada, Phys. Rev. B **55**, 9356 (1997).